Journal of Applied Microbiology

Journal of Applied Microbiology ISSN 1364-5072

ORIGINAL ARTICLE

Synthesis, characterization and antifungal activity of chemically and fungal-produced silver nanoparticles against *Trichophyton rubrum*

L. Pereira[1], N. Dias[1], J. Carvalho[1], S. Fernandes[2], C. Santos[1] and N. Lima[1]

1 CEB—Centre of Biological Engineering, University of Minho, Campus Gualtar, Braga, Portugal
2 Shannon ABC, Limerick Institute of Technology, Moylish Park, Limerick, Ireland

Keywords
antimicrobials, dermatophytes, fungi, infection, mycology.

Correspondence
Nelson Lima, Centre of Biological Engineering, Universidade do Minho, Campus de Gualtar, 4710-057 Braga, Portugal.
E-mail: nelson@ie.uminho.pt

2013/1631: received 11 August 2013, revised 11 September 2014 and accepted 16 September 2014

doi:10.1111/jam.12652

Abstract

Aims: To characterize and explore the potential in extracellular biosynthesis of silver nanoparticles (AgNPs) by *Penicillium chrysogenum* and *Aspergillus oryzae* and to investigate the antifungal effect of chemically *vs* biologically synthesized AgNPs comparing with conventional antifungal drugs against *Trichophyton rubrum*.

Methods and Results: Chemically synthesized AgNPs (Chem-AgNPs) coated with polyvinylpyrrolidone (PVP) were synthesized by chemical reduction method with glucose in PVP aqueous solution. Biologically synthesized AgNPs (Bio-AgNPs) were produced from the extracellular cell-free filtrate of *P. chrysogenum* MUM 03.22 and *A. oryzae* MUM 97.19. Among the commercial antifungal drugs, terbinafine exhibited the lower minimal inhibitory concentration (MIC) range values of 0·063–0·25 μg ml^{-1} for the clinical strains. Chem-AgNPs exhibited antifungal activity against all *T. rubrum* strains. Bio-AgNPs produced by the fungal cell-free filtrate of *P. chrysogenum* showed an antifungal activity higher than fluconazole but less than terbinafine, itraconazole and Chem-AgNPs.

Conclusion: The synthesis parameters in future works should be carefully studied to take full advantage of all the potential of filamentous fungi in the synthesis of AgNPs.

Significance and Impact of the Study: Bio-AgNPs could be used as antifungal agents, namely against dermatophytes.

Introduction

Fungi are a ubiquitous and diverse group of unique organisms. Some groups of fungi are plant pathogens, others can cause severe infections in human beings (Fernandes *et al.* 2013; Pereira *et al.* 2014). Emerging and re-emerging fungal pathogens have been continuously detected and described (Dias *et al.* 2011a; Santos *et al.* 2011). Among humans, the dermatophytoses, which are skin diseases caused by a group of fungi called dermatophytes, have the highest incidence worldwide with an estimation of 20–25% of the population infected (Havlickova *et al.* 2008; Dias *et al.* 2011b). Although the condition is relatively benign and easy to treat, infections caused by dermatophytes are often associated with relapses after antifungal therapy (Gupta and Cooper 2008; Mukherjee *et al.* 2008; Dias *et al.* 2011b). Moreover, dermatophytoses can cause major problems in immunocompromised hosts (Garber 2001; Nir-Paz *et al.* 2003), and some studies have also shown an increasing prevalence of fungal skin infections in patients infected with HIV (Mirmirani *et al.* 2001; Freytes *et al.* 2007). Besides the concern about this upward trend, it is believed that prophylaxis with antifungals may lead to the emergence of resistant strains (Mukherjee *et al.* 2003). Therefore, there is a pressing need to search for a new generation of antifungal agents (Kim *et al.* 2007; Auberger *et al.* 2012).

Among inorganic antimicrobial agents, silver has been employed most widely since ancient times to fight infections. The antibacterial and antiviral activities of silver, silver ions and silver compounds have been thoroughly investigated (Singh *et al.* 2008). Silver is a metal widely used in the pharmaceutical formulations for their antiseptic properties. It has been described that the small size of the silver particles enhances the antimicrobial properties (Toshijazu 1999). Increasing the ratio between the surface area and the volume up to the nanoscale, the antimicrobial effect is amplified; that is, more sites of interaction with biological receptors are available (Lee *et al.* 2003), providing a strong contact with microorganisms surface, thus increasing their antimicrobial efficiency (Rai *et al.* 2009; Thakkar *et al.* 2010; Reidy *et al.* 2013).

Although well-known toxic effects of silver in microorganisms (Sondi and Salopek-Sondi 2004), the mechanisms by which it exerts its bioactivity are still not very well understood or agreed upon (Marambio-Jones and Hoek 2010; Reidy *et al.* 2013). Some studies have reviewed this point in detail attributing the antimicrobial activity of silver to three common mechanisms, namely (i) uptake of free silver ions followed by disruption of ATP production and DNA replication; (ii) generation of reactive oxygen species (ROS) by silver nanoparticles (AgNPs) and silver ion; and (iii) direct disruption of cell membrane integrity by the formation of 'pits' on the membrane surface leading to cell death (Marambio-Jones and Hoek 2010; Reidy *et al.* 2013).

Different sizes and shapes of AgNPs can be easily synthesized by conventional chemical methods (Tran *et al.* 2013), where most of them can present high environmental impact, however. Generally, chemical methods are inexpensive to produce AgNPs on large scale. Nevertheless, most synthetic methods rely heavily on the use of toxic organic solvents and reducing agents (Pastoriza-Santos and Liz-Marzán 2009). All these chemicals are highly reactive and can induce potential environmental and biological contamination (Xu *et al.* 2003; Sui *et al.* 2008). To develop a synthesis process of metal nanoparticles more eco-friendly, the use of natural sources, such as biological systems, becomes essential. A vast array of microbial resources available in nature can be employed as an alternative to the use of hazardous chemicals for AgNPs synthesis (Thakkar *et al.* 2010).

Different micro-organisms have different mechanisms of producing nanoparticles (Li *et al.* 2011). However, in the biological approach, it has been suggested that biomolecules, secreted in large amounts by micro-organisms, are involved in the reduction of metal ions, thus controlling the size of the nanoparticles (Kumar *et al.* 2007; Thakkar *et al.* 2010). There are some advantages of biological over chemical synthesis of nanoparticles. The manipulation of microbial cultures is easy, and the actual refining process of the biomass is simpler in comparison with synthetic methods (Ingle *et al.* 2008). Biosynthetic nanoparticles have a lower environmental impact because their synthesis does not require any toxic chemical, and also, the synthesis process occurs at ambient temperature and ambient pressure conditions (Gade *et al.* 2008; Mukherjee *et al.* 2008). The use of fungi is potentially interesting because they exhibit tolerance and metal bioaccumulation potential and secrete large amounts of enzymes and the scale-up synthesis of nanoparticles to a larger scale is easier (Rai *et al.* 2011). Consequently, biological approach has shown to be cost-effective, simpler and focus towards a greener approach (Maliszewska 2011).

Several studies have reported potent antifungal activity of AgNPs against pathogenic fungi, and most of them have been focused on the effect of AgNPs on the *Candida* species (Chwalibog *et al.* 2010; Monteiro *et al.* 2011; Nasrollahi *et al.* 2011; Hwang *et al.* 2012; Rajarathinam and Kalaichelvan 2013). However, only few studies have been performed to assess the effects of AgNPs on dermatophytes. The antifungal activity of AgNPs in biostabilized footwear materials was evaluated against dermatophytes and other fungi (Falkiewicz-Dulik and Macura 2008). Chemically synthesized AgNPs (Chem-AgNPs) shown antifungal activity against clinical isolates of *Trichophyton mentagrophytes* (Kim *et al.* 2008). Noorbakhsh (2011) investigated the effects of biologically synthesized AgNPs (Bio-AgNPs) by *Klebsiella pneumoniae* against *Trichophyton rubrum*. In addition, Marcato *et al.* (2012) have also reported the significant antifungal activity of Bio-AgNPs against *T. rubrum* by the disc diffusion test.

The main aims of this study were (i) to explore the potential in extracellular biosynthesis of Bio-AgNPs by different filamentous fungi, (ii) characterize the obtained Bio-AgNPs and chemically synthesized AgNPs (Chem-AgNPs), (iii) evaluate the antifungal effect of Chem-AgNPs *vs* Bio-AgNPs and (iv) compare the performance of both AgNPs with conventional antifungal drugs.

Materials and methods

Fungal strains

In this work, the fungi *Penicillium chrysogenum* MUM 03.22, *Aspergillus oryzae* MUM 97.19 and eight clinical strains of *T. rubrum* MUM 08.05; 08.09; 08.10; 08.11; 08.12; 09.18; 10.128 and 10.133 were obtained from the Portuguese fungal culture collection *Micoteca da Universidade do Minho* (MUM, Braga, Portugal). The reference strain *T. rubrum* ATCC MYA-4438 was obtained from

the American Type Culture Collection (ATCC—LGC Standards S.L.U., Barcelona, Spain).

Chem-AgNPs

Chem-AgNPs coated with polyvinylpyrrolidone (PVP) were synthesized with some modifications by chemical reduction method with glucose in PVP aqueous solution as described elsewhere (Wang *et al.* 2005). Briefly, 2 g of glucose (Fluka: Buchs, Switzerland) and 1 g PVP 10 000 g mol^{-1} (Sigma-Aldrich: St. Louis, MO, USA) were dissolved into 40 ml of Milli-Q deionized water (solution A). The silver aqueous solution was prepared by dissolving 0·5 g of $AgNO_3$ (Sigma: Sigma-Aldrich, St. Louis, MO, USA) in 1 ml of Milli-Q deionized water (solution B). Solution A was heated to 70°C under continuous stirring. When thermometer registered 70°C, solution B was then added dropwise to solution A with a flow rate 1 drop/s and continuous stirring. The dispersion was maintained at 70°C for 1 h and then cooled to room temperature. The particles were separated from oxidation products, glucose, PVP, $AgNO_3^-$ and Ag^+ by centrifugation (5000 ***g***, 5 min).

Bio-AgNPs

For the biosynthesis of AgNPs, the methodologies presented by Ahmad *et al.* (2003) and Durán *et al.* (2005) were taken into consideration. However, some modifications were put in place, as follows. Fungal cells were grown in glucose-yeast extract-peptone (MGYP) liquid medium (0·3% malt extract, 1% glucose, 0·3% yeast extract and 0·5% peptone) and incubated at 30°C with 150 rev min^{-1} for 72 h. The fungal biomass was then harvested followed by extensive washing with Milli-Q deionized water. In a glass flask, 10 g (wet weight of biomass) was added to 100 ml of Milli-Q deionized water and incubated with shaking for 72 h (30°C at 150 rev min^{-1}). Afterwards, the fungal biomass in the aqueous suspension was filtered through a Whatman grade 1 filter paper (Whatman: Buckinghamshire, UK), and the fungal filtrate was finally obtained.

Biosynthesis of Bio-AgNPs was achieved by adding 1 mmol l^{-1} $AgNO_3$ to 100 ml of the fungal filtrate, which was incubated in the dark at 30°C and 150 rev min^{-1} for 96 h. Control flask, without the $AgNO_3$, was incubated at same conditions. Aliquots of the reaction solution were taken at 96 h of incubation for characterization of Bio-AgNPs by Ultraviolet-Visible (UV/VIS) spectrophotometer analysis and dynamic light scattering (DLS). The remaining aqueous solution containing Bio-AgNPs (reaction solution) was purified by repeated centrifugation at 5000 ***g*** for 15 min followed by redispersion of the pellet of Ag-NPs in Milli-Q deionized water. After freeze-drying, the samples were ready for further analysis by X-ray diffraction (XRD), Fourier transform infrared (FT-IR) and scanning electron microscopy (SEM/EDS).

Ultraviolet-Visible Spectroscopy

The detection of silver nanoparticles was performed by UV/VIS spectrophotometer (V-560 Jasco: Tokyo, Japan) equipped with a double-beam system and double monochromator, in a wavelength ranging 200–800 nm at a resolution of 1 nm, for each sample.

Dynamic light scattering

The size distribution and the polydispersity of the AgNPs were studied by DLS technique. A sample of 1 ml of the reaction solution was placed in disposable plastic cuvettes, and the hydrodynamic diameter of the AgNPs was measured in the Malvern Instrument Zetasizer Nano ZS (Malvern, UK). Measurements were taken at 25°C in triplicate.

Scanning electron microscopy

Morphological characterization and elemental analysis of Bio-AgNPs were performed with an ultrahigh-resolution field emission scanning electron microscope (NanoSEM —FEI Nova 200—FEG/SEM: OR, USA), with integrated microanalysis X-ray system (energy dispersive spectrometer (EDS)) and electron backscatter diffraction (EBSD, EDAX—Pegasus X4M (EDS/EBSD)). For SEM analysis, a portion of freeze-dried of each Chem-AgNPs and Bio-AgNPs was loaded in the specimen holder of the equipment and afterwards analysed.

X-ray diffraction

The structure and composition of freeze-dried Chem-AgNPs and Bio-AgNPs were analysed by XRD equipment (Bruker D8 Discover: Karlsruhe, Germany) operated at a voltage of 40 kV adjustable in steps of 1 kv with a θ- 2 θ configuration and Cu Kα radiation (λ = 1·5406 Å). The diffracted intensities were recorded from 30° to 80° 2θ angles.

FT-IR analysis

The interaction between polymeric structure of PVP with Chem-AgNPs and proteins with Bio-AgNPs in freeze-dried samples was analysed by FT-IR using a Bruker IFS 66V equipment (Bruker) in a wavelength ranging from

4000 to 500 cm^{-1}. For comparison purpose, FT-IR spectrum of pure PVP 10 000 g mol^{-1} was obtained from the open Japanese database 'Spectral Database for Organic Compounds, SDBS', a free database of the National Institute of Advanced Industrial Science and Technology (AIST), Japan (http://sdbs.db.aist.go.jp/sdbs/cgi-bin/cre_index.cgi—date of access: 09 June 2014).

Susceptibility tests to antifungal agents

Antifungal drugs

Commercial antifungal terbinafine hydrochloride (>98%; Sigma-Aldrich), itraconazole (>98%, TLC; Sigma-Aldrich) and fluconazole (>98%, HPLC; Sigma-Aldrich) were used as reference drugs. A stock solution of antifungal drugs was prepared at concentrations 100 times the highest concentration tested for each antifungal drug. Terbinafine and itraconazole were dissolved in DMSO, and fluconazole was dissolved in distilled water. Aliquots were prepared and stored at −80°C. The concentration ranges used were 0·0078–4 μg ml^{-1} for terbinafine, 0·0313–16 μg ml^{-1} for itraconazole and 0·125–64 μg ml^{-1} for fluconazole. Final concentration of DMSO never exceeded 1% of the final concentration of drugs, even in the control (without antifungal drug).

Concentration of AgNPs

For susceptibility test, freeze-dried of Chem- and Bio-AgNPs was dispersed by ultra-sonication in Milli-Q deionized water to produce a stock solution with the final concentration of 20 μg mol^{-1}. Then, the stock solution was diluted in RPMI-1640 medium (with glutamine, without bicarbonate and with phenol red as pH indicator) buffered to pH 7·0 ± 0·1 at 25°C, supplemented with 10% foetal bovine serum (FBS) (Invitrogen: Carlsbad, CA, USA) to produce work solutions with the following concentrations: 0·25, 0·5, 1·0, 2·0, 2·5, 3·0, 3·5, 4·0, 5·0 and 7·5 μg ml^{-1}.

Susceptibility test procedure

Clinical and ATCC MYA-4438 strains of *T. rubrum* were grown at 30°C for 7–10 days in potato dextrose agar slants (PDA; Oxoid, UK). The procedure followed the Clinical and Laboratory Standards Institute document M38-A2 (CLSI 2008).

A serial concentration of each antifungal drugs and AgNPs was used in the range described above. The inoculum size was set in a range of $0{\cdot}4 \times 10^4$ to 5×10^4 CFU ml^{-1}. The microdilution plates inoculated with 100 μl of fungal conidia were incubated at 30°C, and the turbidity of the growth control wells was observed every 48 h. The minimal inhibitory concentration (MIC) of each strain was defined as the lowest concentration that inhibited 80% of the fungal growth and was determined by a comparison with the fungal growth in the control well.

Results

Characterization of Chem-AgNPs and Bio-AgNPs

During reduction reaction, the reaction solution of Chem-AgNPs changed from translucent white to dark brown. For Bio-AgNPs, the reaction solution changed from pale yellow to dark brown. No changing of colour was observed neither in the control flasks, containing only Milli-Q deionized water supplemented with 1 mmol l^{-1} $AgNO_3$, nor in the fungal filtrate without $AgNO_3$ (data not shown).

The reduction reaction of the silver ion (Ag^+) to the silver metal (Ag^0) was monitored by UV/VIS spectrophotometry. A unique spectral response was displayed at 430 nm for Chem-AgNPs (data not shown). In Fig. 1, the UV/VIS spectrum of Bio-AgNPs produced by *P. chrysogenum* MUM 03.22 showed a single peak at 430 nm, but a wide band in the range between 400 and 550 nm was observed for Bio-AgNPs produced by *A. oryzae* MUM 97.19. No absorption band was observed on the spectra of blank solution.

The physicochemical properties such as size distribution and polydispersity index were analysed by DLS (Table 1). The size distribution of Chem-AgNPs was

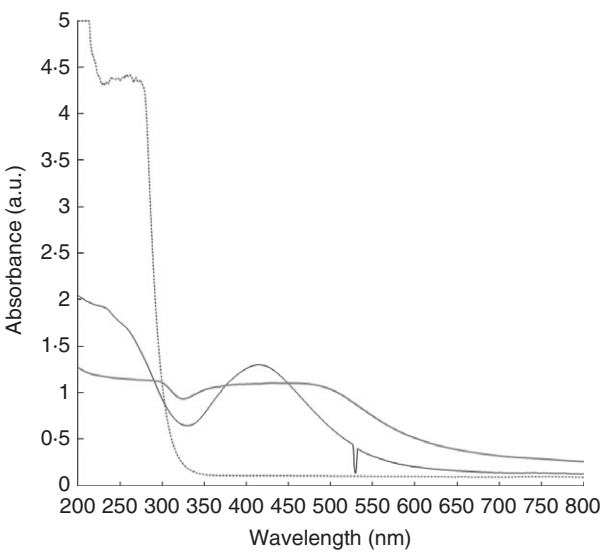

Figure 1 UV/VIS spectrum after 96 h of $AgNO_3$ reduction by reaction solution of *Penicillium chrysogenum* MUM 97.19 (black line) and *Aspergillus oryzae* MUM 03.22 (grey line). Blank represents the cell-free filtrate without $AgNO_3$ (dashed line).

Table 1 Physicochemical parameters of size distribution and polydispersion value for Chem-AgNPs, and Bio-AgNps produced by *Penicillium chrysogenum* MUM 03.22 and *Aspergillus oryzae* MUM 97.19 cell-free filtrate

	Z—average size (nm)	Polydispersion	Distribution
Chem-AgNPs	73·72	0·254	Unimodal
Bio-AgNPs *P. chrysogenum* MUM 03.22	100·6	0·230	Bimodal
Bio-AgNPs *A. oryzae* MUM 97.19	76·14	0·377	Bimodal

found to be monomodal, with average particle size of 73·72 nm and polydispersity of 0·254. In contrast, a bimodal size distribution was found for Bio-AgNPs produced by *P. chrysogenum* MUM 03.22 with average particle size of 100·6 nm. A polydispersity index of 0·230 was also observed for these nanoparticles. Bio-AgNPs produced by *A. oryzae* MUM 97.19 showed a bimodal size distribution with average particle size of 76·14 nm and a polydispersity index of 0·377.

Each Chem-AgNPs and Bio-AgNPs obtained were also characterized by SEM analysis (Fig. 2). The representative SEM micrograph recorded from a drop-coated film of Chem-AgNPs deposited on a carbon-coated copper grid is displayed in Fig. 2a. Variable shapes (spherical to polyhedric particles) formed with size ranging from 25 to 75 nm were observed. The average particle size diameter of spherical Chem-AgNPs was 52 nm although some aggregates were also present. In contrast, micrographs taken from Bio-AgNPs synthesized by *P. chrysogenum* MUM 03.22 and by *A. oryzae* MUM 97.19 (Fig. 2b,c, respectively) showed mostly spherical-shaped nanoparticles formed with diameters ranging from 19 to 60 nm. To provide confirmation on the presence of silver ions in the solution, analysis on SEM-EDS was recorded (Fig. 3). A peak of metallic copper that was found for Chem-AgNPs (Fig. 3a) was generated from the carbon-coated copper grid and did not account for the final analysis. The EDS optical absorption peak was observed approximately at 3 keV, indicating the presence of AgNPs in the reaction solution of *P. chrysogenum* MUM 03.22 and *A. oryzae* MUM 97.19, respectively (Fig. 3b,c).

FT-IR spectroscopy is a suitable and sensitive method to characterize and detect the interaction between two chemical species. The FT-IR spectra for Chem-AgNPs and Bio-AgNPs are displayed in Fig. 4a–c. The infrared spectra of both pure e and PVP-capped AgNPs are quite different. The C=O groups of pure PVP show a prominent band at 1663 cm^{-1} in the infrared spectrum (data not shown). This characteristic band can be subjected to a shift when an interaction between PVP and metal spe-

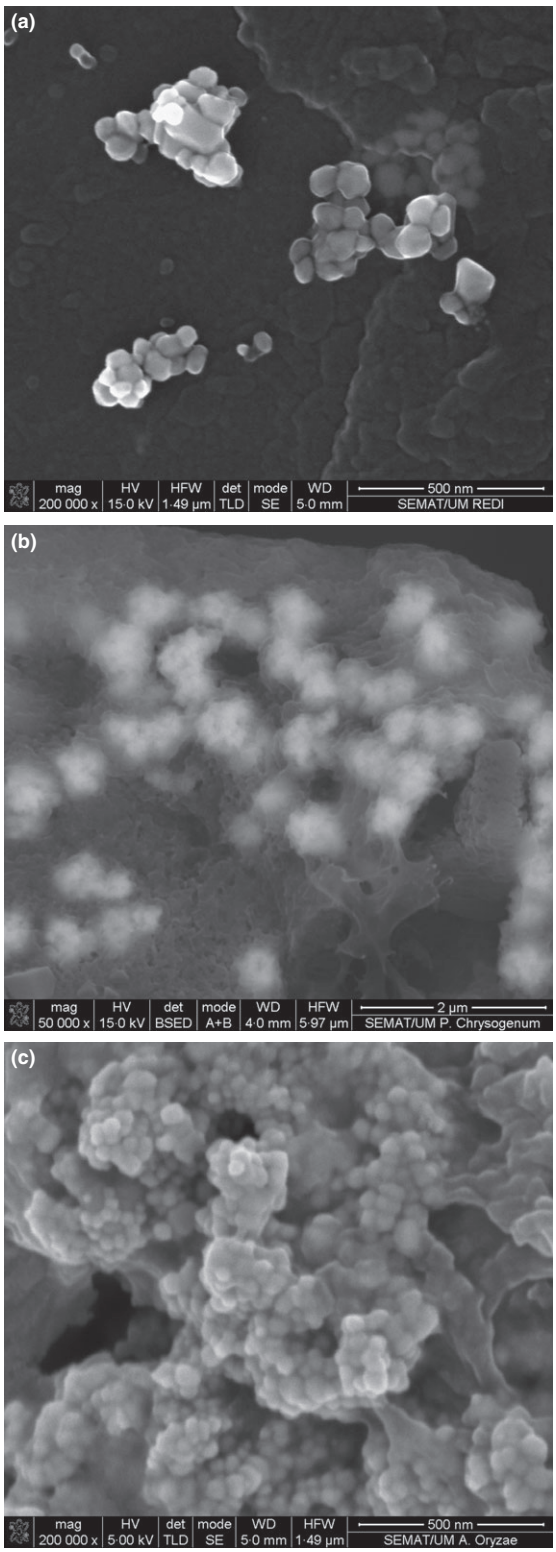

Figure 2 Representative scanning electron microscopy (SEM) micrograph of (a) Chem-AgNPs, (b) Bio-AgNPs synthesized by *Penicillium chrysogenum* MUM 97.19 and (c) Bio-AgNPs synthesized by *Aspergillus oryzae* MUM 03.22.

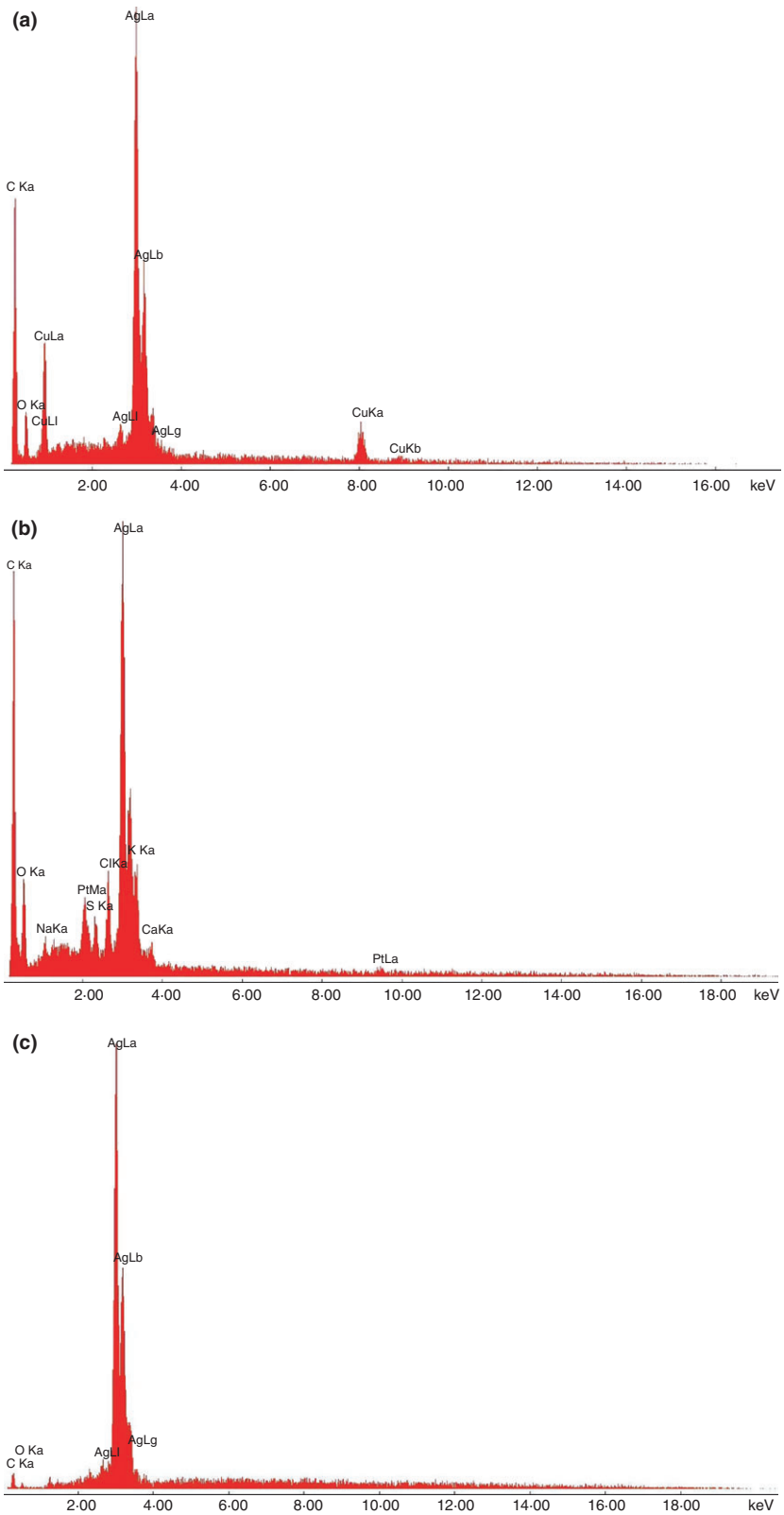

Figure 3 Energy dispersive spectrometer (EDS) spectrum of (a) Chem-AgNPs, (b) Bio-AgNPs synthesized by *Penicillium chrysogenum* MUM 97.19 and (c) Bio-AgNPs synthesized by *Aspergillus oryzae* MUM 03.22.

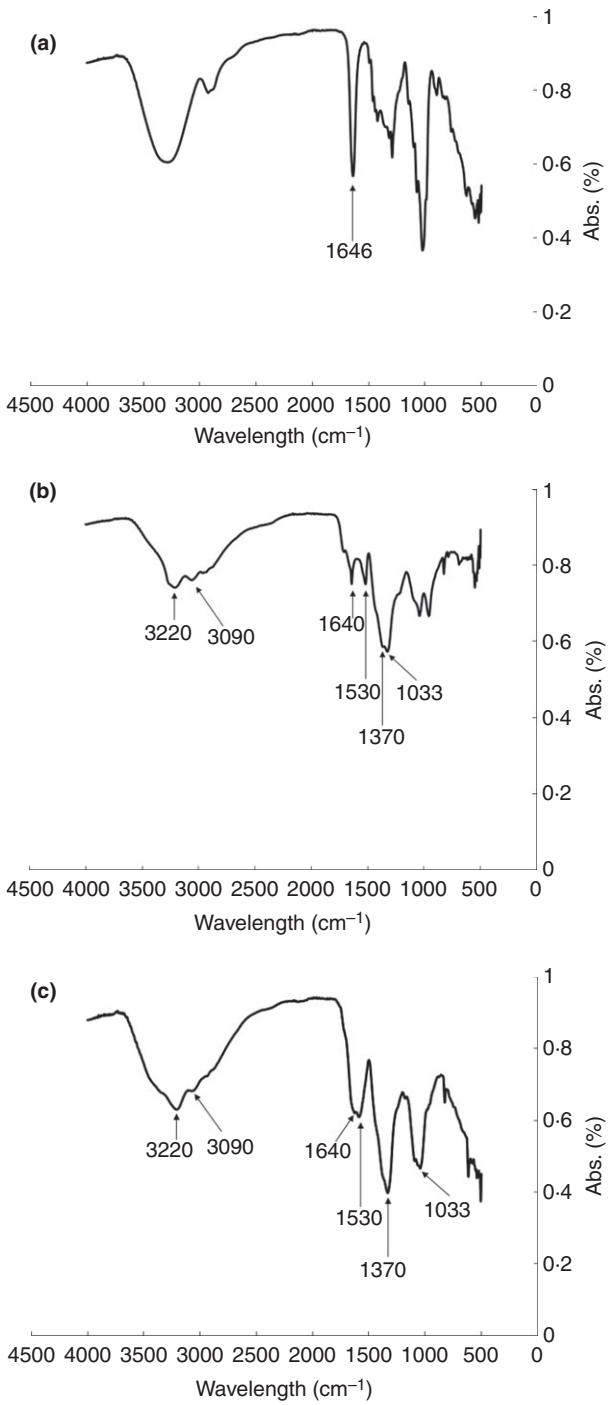

Figure 4 Fourier transform infrared (FT-IR) spectrum of (a) Chem-AgNPs, (b) Bio-AgNPs synthesized by *Penicillium chrysogenum* MUM 97.19 and (c) Bio-AgNPs synthesized by *Aspergillus oryzae* MUM 03.22.

cies occur (Tu 2008). In this study, this shift was observed for the C=O group of PVP-capped Chem-AgNPs. In this case, a band at 1646 cm^{-1} was observed (Fig. 4a). The band shifts reveal that there exists an interaction between metal precursors and PVP.

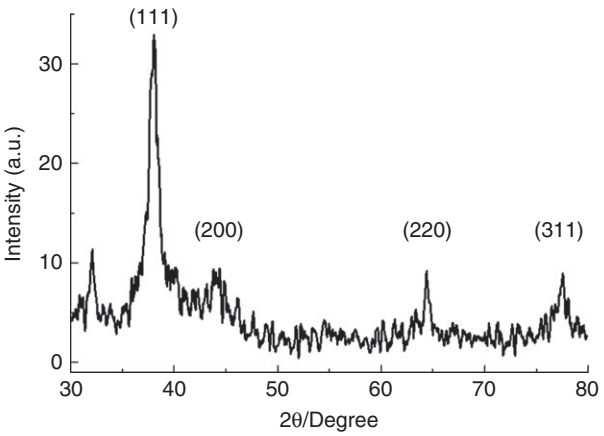

Figure 5 Example of representative X-ray diffraction pattern of freeze-dried silver nanoparticles synthesized by the reduction of silver nitrate with *Penicillium chrysogenum* MUM 97.19 cell-free filtrate (a.u. = arbitrary units).

The infrared spectra of both Bio-AgNPs produced by *P. chrysogenum* MUM 03.22 and *A. orizae* MUM 97.19 presented bands seen at 3220 cm^{-1} with a shoulder at 3090 cm^{-1}, which were assigned to the stretching vibrations of primary and secondary amines, respectively (Fig. 4b,c). Their corresponding bending vibrations were seen at 1640 and 1530 cm^{-1}, respectively. The two bands observed at 1370 and 1033 cm^{-1} can be assigned to the C–N stretching vibrations of aromatic and aliphatic amines, respectively. Based on the infrared data, overall observation confirms the presence of protein in the samples of both Bio-AgNPs. It was reported earlier that proteins can bind to nanoparticles either through free amine groups or cysteine residues in the proteins (Vigneshwaran *et al.* 2007).

The crystalline structure of Bio-AgNPs synthesized *P. chrysogenum* MUM 03.22 was confirmed by the XRD pattern corresponding to the (111), (200), (220) and (311) planes at 2θ angles of 38·08°, 44·28°, 64·48° and 77·48°, respectively (Fig. 5). The obtained XRD pattern was in good agreement with the unit cell of the face-centred cubic (fcc) structure of synthetic silver (ICSD File No. 01-089-3722) with a lattice parameter of a = 4·0855 Å. Other diffraction peaks were also observed at 2θ angles of 32·08°, 46·00°, 54·6° and 57·3° in the XRD profile. This might be related to silver chloride and silver oxide involved during the preparation of the cell-free filtrate.

Susceptibility tests

In this study, antifungal susceptibility of the eight clinical strains of *T. rubrum* and the reference strain *T. rubrum* ATCC MYA-4438 were tested against three commercial antifungal drugs (terbinafine, itraconazole and fluconaz-

Table 2 Minimum inhibitory concentrations (MICs) of antifungal commercial drugs, Chem- and Bio-AgNPs on clinical and reference strain of *Trichophyton rubrum*

Species (Number of isolates)	Antifungal agents	MIC (μg ml^{-1})	
		Range	Geometric mean
T. rubrum Clinical strains (8)	Terbinafine	0·063–0·25	0·14
	Itraconazole	0·063–1	0·18
	Fluconazole	1–32	5·65
	Chem-AgNPs	0·5–2·5	1·19
	Bio-AgNPs (*Penicillium chrysogenum* MUM 03.22)	0·5–5	2·89
	Bio-AgNPs (*Aspergillus oryzae* MUM 97.19)	>7·5	>7·5
T. rubrum ATCC MYA 4438	Terbinafine	4	nd
	Itraconazole	0·063–0·126	nd
	Fluconazole	0·5–16	nd
	Chem-AgNPs	<0·25	nd
	Bio-AgNPs (*P. chrysogenum* MUM 03.22)	0·5	nd
	Bio-AgNPs (*A. oryzae* MUM 97.19)	>7·5	nd

nd, not determined.

ole), and Chem-AgNPs and Bio-AgNPs produced by *P. chrysogenum* MUM 03.22 and *A. oryzae* MUM 97.19.

To determine the MIC, the plates were evaluated after 5 days of incubation (Table 2). The reference strain *T. rubrum* ATCC MYA-4438 was the most susceptible fungus against itraconazole, fluconazole, Chem-AgNPs and Bio-AgNPs. In contrast, it was the less susceptible to terbinafine. Among the commercial antifungal drugs evaluated, terbinafine exhibited the lower MICs values (0·063–0·25 μg ml^{-1}) for all clinical strains.

Chem-AgNPs showed antifungal activity in the range from 0·25 to 2·5 μg ml^{-1}. Furthermore, Chem-AgNPs exhibited a stronger inhibitory effect against all *T. rubrum* strains evaluated, which MIC values were at least twofold higher than the MIC values of Bio-AgNPs (data not shown).

Bio-AgNPs produced by *P. chrysogenum* MUM 03.22 showed an antifungal activity in the range from 0·5 to 5·0 μg ml^{-1}. The Bio-AgNPs produced by that fungi exhibited higher antifungal activity than fluconazole, but lower activity than terbinafine, itraconazole and Chem-AgNPs. In contrast, Bio-AgNPs produced by *A. oryzae* MUM 97.19 did not exhibit antifungal activity in concentrations up to 7·5 μg ml^{-1}. Regardless of the process used, Chem-AgNPs and Bio-AgNPs produced by *P. chrysogenum* MUM 03.22 (geometric mean of MIC values = 1·19 and 2·89 μg ml^{-1}, respectively) exhibited a stronger inhibiting activity than fluconazole (geometric mean of MIC values = 5·65 μg ml^{-1}).

Discussion and conclusion

Nanoparticle biosynthesis using filamentous fungi has recently emerged as a simple and viable alternative to those procedures involving the physicochemical synthetic route (Hemath *et al.* 2010). In the present study, the synthesis and antifungal activity of both Chem-AgNPs and Bio-AgNPs were assessed. Chem-AgNPs were colloidally stabilized by the polymer PVP (10 000 g mol^{-1}). The UV/VIS spectrum for this sample resulted in a maximum absorption band at 430 nm, which was in accordance with previous studies (Kittler *et al.* 2010; Racles *et al.* 2010). The Chem-AgNPs were stable after 3 months, once no precipitation was observed and the solution containing it was evaluated by UV/VIS and no changing was registered over the time (data not shown).

The fungal strains *P. chrysogenum* MUM 03.22 and *A. oryzae* MUM 97.19 were used as biological models for the extracellular biosynthesis of stable Bio-AgNPs. After silver nitrate addition to the fungal cell-free filtrate, the colour of the reaction solution changed over the time of incubation, which indicated the formation of Bio-AgNPs. According to previous published data, the changing in the reaction solution colour is due to the excitation of surface plasmon vibrations in the Bio-AgNPs (Mulvaney 1996; Elechiguerra *et al.* 2005). Furthermore, the absorbance band between 380 and 420 nm indicates the formation of spherical or roughly spherical Bio-AgNPs (Hasell *et al.* 2007; Pal *et al.* 2007).

Differences were found between UV/VIS spectra of Bio-AgNPs. For nanoparticles produced by *P. chrysogenum* MUM 03.22, a plasmon resonance band at 420 nm was obtained. The wide band observed on the spectrum of Bio-AgNPs produced by *A. oryzae* MUM 97.19 indicated a heterogeneous suspension. An absorption band at 270 nm was also found on both Bio-AgNPs spectra. This band is attributed to the electronic excitation of both aromatic tyrosine and tryptophane residues in proteins (Lakowicz 2006). It indicates the presence of extracellu-

lar proteins in the filtrate solution and the possible involvement of the amino acids in the reduction and stability of metallic ions (Mandal *et al.* 2006). The presence of proteins in Bio-AgNPs was confirmed by the FT-IR analyses. FT-IR measurements of the freeze-dried samples were taken to identify the possible interactions between silver and bioactive molecules, which may be responsible for stabilization of AgNPs. The amide linkages between amino acid residues in proteins lead to well-known signatures in the infrared region of the electromagnetic spectrum. FT-IR spectrum reveals two bands at 3207 and 3065 cm^{-1} that corresponds to stretching vibrations of the amide primary and secondary bands of the proteins, respectively. The presence of the signature peaks of amino acids supports the presence of proteins in fungal cell-free filtrate as observed in UV/VIS spectra.

The SEM micrographs show the high density of nanostructures, confirming the presence of Chem-AgNPs and Bio-AgNPs. Differences in the average size of Chem-AgNPs and Bio-AgNPs were found comparing DLS and SEM analyses. Results from DLS suggested an average size of almost twofold for Bio-AgNPs than Chem-AgNPs. In fact, DLS technique measures the hydrodynamic diameter of the particle. It gives the information of the inorganic core along with any coating material and the solvation layer attached to the particle. It means that nanomaterial sizing determined by techniques that use wet dispersion is commonly overestimated (De Palma *et al.* 2007; Dhawan and Sharma 2010). In contrast, SEM analysis uses dehydrated samples, where only the inorganic core and the coating material were taken into account. In addition, due to poor contrast, the measurement of the coating layer can sometimes be underestimated (Gaumet *et al.* 2008).

A thick cap surrounding the nanoparticles could be observed in SEM micrographs. This is probably due to the biomolecules released from the fungus (Durán *et al.* 2005) acting as stabilizing agents of the nanoparticles. The absorption peak on SEM-EDS was observed at approximately 3 keV, which is characteristic of silver nanocrystals. The presence of other peaks besides silver products in the EDS spectra indicated the heterogeneity of the reaction solution.

The development of a protocol to synthesize AgNPs with controlled size and shape is critical (Birla *et al.* 2013). In fact, it has been reported that the shape of AgNPs may interfere with their antimicrobial effect (Pal *et al.* 2007). Recent studies have confirmed that metal nanomaterial has good antimicrobial activity and among inorganic agents, silver has been most widely employed since ancient times (Jung *et al.* 2008).

The biological activity of Chem-AgNPs and Bio-AgNPs was evaluated against eight clinical strains of *T. rubrum* and reference strain *T. rubrum* ATCC MYA-4438. The differences between the MIC values of Chem-AgNPs and Bio-AgNPs produced by *P. chrysogenum* MUM 03.22 can be in part explained by the size ranges of the nanoparticle, as the smaller sized Chem-AgNPs exhibited lower MIC range than Bio-AgNPs. Previous studies indicated that size and shape of AgNPs have a direct implication on potential toxicity (Singh *et al.* 2008; De Lima *et al.* 2012). Therefore, the presence of uncapped Ag^0 nanoparticles in the Chem-AgNPs suspension could exhibit *per se* high toxicity (Pal *et al.* 2007; Kvitek *et al.* 2009; Kittler *et al.* 2010). However, AgNPs with smaller sizes have a higher antimicrobial activity, as smaller particles with a larger surface-to-volume ratio provide a more efficient means of antimicrobial activity (Baker *et al.* 2005; Panáček *et al.* 2009; Durán *et al.* 2010).

Reduced antifungal activity against clinical and reference *T. rubrum* strains of the reaction solution of *A. oryzae* MUM 97.19 could be associated with the coating of the nanoparticles, and the results suggested that the biomolecules coating the AgNPs might play an important role in the antimicrobial effect. Our results suggested that AgNPs capping might also be involved in the antifungal activity, because Chem-AgNPs which was only covered with PVP exhibited higher biological activity against *T. rubrum* strains than the biological capping of AgNPs produced by fungi. Irrespective of the process used, Chem- and Bio-AgNPs exhibited at least tenfold stronger inhibiting activity against dermatophytes than fluconazole. This result is in accordance with Kim *et al.* (2008), who reported that AgNPs shown higher activity than fluconazole towards all fungal strains tested, including *T. mentagrophytes*.

For susceptibility tests involving AgNPs, the stabilization of AgNPs in the culture medium is required, besides the agglomeration of AgNPs can greatly compromise their antimicrobial activity (Lok *et al.* 2007). So it is recommended performing agglomeration tests to understand and monitor the stabilization of AgNPs in culture medium (Kittler *et al.* 2010). In our study, the presence of salts in the RPMI medium interfered with the stabilization of the Chem-AgNPs leading to their agglomeration (data not shown). The PVP capping of the Chem-AgNPs was undertaken to enable a more effective redispersion and reduced propensity towards aggregations by steric hindrance (Kvitek *et al.* 2008). It is known that capping agents increase the solubility of the nanosystem, being also used as a site for bioconjugation of the nanoparticle with important molecules (Sing *et al.* 2009; Seabra and Durán 2010). The PVP capping of Chem-AgNPs was confirmed by FT-IR analysis comparing IR spectra of pure PVP 10 000 g mol^{-1} and PVP-capped Chem-AgNPs. The characteristic band of the C=O groups at 1663 cm^{-1} (pure PVP) can be subjected to a shift when an interaction between PVP and metal species occur (Tu 2008). In the present study, a band at 1646 cm^{-1} was

observed for Chem-AgNPs capped with PVP. The band shifts reveal an interaction between metal precursors and PVP. Based on the IR data, overall observation confirms the presence of protein in the samples of both Bio-AgNPs. It was reported earlier that proteins can bind to nanoparticles through either free amine groups or cysteine residues in the proteins (Vigneshwaran *et al.* 2007).

The antifungal drug terbinafine has shown higher antifungal activity than all Chem- and Bio-AgNPs; nevertheless, the terbinafine-resistant strain ATCC MYA-4438 was susceptible to nanoparticles exposition, which antifungal mechanism of action is different than the commercial drug. It is known that conventional antifugal treatments have limitations associated with their toxicity, antifungal resistance, relapses and high treatment costs (Khan *et al.* 2010). The presence of clinical isolates of terbinafine-resistant *T. rubrum* exhibiting high-level primary resistance to terbinafine, which is one of the most used antifungal drugs (Mukherjee *et al.* 2003; Favre *et al.* 2004), reinforces the issue that resistance to antifungal drugs represents an important impact in the management of fungal diseases. Notwithstanding the reduced antifungal activity of the strain *A. oryzae* MUM 97.19, promising results were found for the Bio-AgNPs produced from the cell-free filtrate of *P. chrysogenum* MUM 03.22.

The synthesis parameters in future studies should be carefully studied to take full advantage of all the potential of filamentous fungi in the synthesis of Bio-AgNPs, which revealed as potential antifungal agent, that could help to prevent superficial cutaneous fungal infections.

Acknowledgements

The authors thank Pedro Martins (Physics Department of University of Minho) for help in XRD analysis. The authors thank to SDBSWeb: http://sdbs.db.aist.go.jp (Japanese National Institute of Advanced Industrial Science and Technology). The authors thank the FCT Strategic Project PEst-OE/EQB/LA0023/2013. Nicolina Dias acknowledges the project 'Consolidating Research Expertise and Resources on Cellular and Molecular Biotechnology at CEB/IBB', RECI/BBB-EBI/0179/2012.

Conflict of Interest

The authors have no conflict of interest to declare.

References

Ahmad, A., Mukherjee, P., Senapati, S., Mandal, D., Khan, M.I., Kumar, R. and Sastry, M. (2003) Extracellular biosynthesis of silver nanoparticles using the fungus *Fusarium oxysporum*. *Colloids Surf B Biointerfaces* **28**, 313–318.

Auberger, J., Lass-Flörl, C., Aigner, M., Clausen, J., Gastl, G. and Nachbaur, D. (2012) Invasive fungal breakthrough infections, fungal colonization and emergence of resistant strains in high-risk patients receiving antifungal prophylaxis with posaconazole: real-life data from a single-centre institutional retrospective observational study. *J Antimicrob Chemother* **67**, 2268–2273.

Baker, C., Pradhan, A., Pakstis, L., Pochan, D.J. and Shah, S.I. (2005) Synthesis and antibacterial properties of silver nanoparticles. *J Nanosci Nanotechnol* **5**, 244–249.

Birla, S.S., Gaikwad, S.C., Gade, A.K. and Rai, M.K. (2013) Rapid synthesis of silver nanoparticles from *Fusarium oxysporum* by optimizing physicocultural conditions. *ScientificWorldJournal* **2013**. http://dx.doi.org/10.1155/2013/796018.

Chwalibog, A., Sawosz, E., Hotowy, A., Szeliga, J., Mitura, S., Mitura, K., Grodzik, M., Orlowski, P. *et al.* (2010) Visualization of interaction between inorganic nanoparticles and bacteria or fungi. *Int J Nanomed* **5**, 1085–1094.

CLSI (2008) *Reference Method for Broth Dilution Antifungal Susceptibility Testing of Filamentous Fungi; Approved Standard CLSI Document M38–A2*. Wayne: Clinical and Laboratory Standards Institute.

De Lima, R., Seabra, B.A. and Durán, N. (2012) Silver nanoparticles: a brief review of cytotoxicity and genotoxicity of chemically and biogenically synthesised nanoparticles. *J Appl Toxicol* **32**, 867–879.

De Palma, R., Peeters, S., Van Bael, M.J., Van den Rul, H., Bonroy, K., Laureyn, W., Mullens, J., Borghs, G. *et al.* (2007) Silane ligand exchange to make hydrophobic superparamagnetic nanoparticles water dispersible. *Chem Mater* **19**, 1821–1831.

Dhawan, A. and Sharma, V. (2010) Toxicity assessment of nanomaterials: methods and challenges. *Anal Bioanal Chem* **398**, 589–605.

Dias, N., Oliveira, M.M.E., Portela, M., Santos, C., Zancope-Oliveira, R.M. and Lima, N. (2011a) Human sporotrichosis caused by *Sporothrix mexicana* in a Portuguese patient. *Emerg Infect Dis* **17**, 1975–1976.

Dias, N., Santos, C., Portela, M. and Lima, N. (2011b) Toenail onychomycosis in a Portuguese geriatric population. *Mycopathologia* **172**, 55–61.

Durán, N., Marcato, P., Alves, O.L., De Sousa, G.I.H. and Esposito, E. (2005) Mechanistic aspects of biosynthesis of silver nanoparticles by several *Fusarium oxysporum* strains. *J Nanobiotechnol* **3**, 1–7.

Durán, N., Marcato, P., De Conti, R., Alves, O.L., Costa, F.T.M. and Brocchib, M. (2010) Potential use of silver nanoparticles on pathogenic bacteria, their toxicity and possible mechanisms of action. *J Braz Chem Soc* **21**, 949–959.

Elechiguerra, J., Burt, J., Morones, J., Camacho-Bragado, A., Gao, X., Lara, H. and Yacaman, M.J. (2005) Interaction of silver nanoparticles with HIV-1. *J Nanobiotechnol* **3**, 1–6.

Falkiewicz-Dulik, M. and Macura, A.B. (2008) Nanosilver as substance biostabilising footwear materials in the foot mycosis prophylaxis. *Mikologia Lekarska* **15**, 145–150.

Favre, B., Ghannoum, M.A. and Ryder, N.S. (2004) Biochemical characterization of terbinafine-resistant *Trichophyton rubrum* isolates. *Med Mycol* **42**, 525–529.

Fernandes, S., Simões, M., Dias, N., Santos, C. and Lima, N. (2013) Fungicidal activity of microbicides. In *Russell, Hugo & Ayliffe's: Principles and Practice of Disinfection, Preservation and Sterilization*, 5th edn. ed. Fraise, A.P., Maillard, J.-Y. and Sattar, S.A. (Org.). pp. 142–154. Oxford, England, UK: Wiley-Blackwell.

Freytes, D.M., Arroyo-Novoa, C.M., Figueroa-Ramos, M.I., Ruiz-Lebrón, R.B., Stotts, N.A. and Busquets, A. (2007) Skin disease in HIV-positive persons living in Puerto Rico. *Adv Skin Wound Care* **20**, 149–156.

Gade, A., Bonde, P., Ingle, A., Marcato, P., Durán, N. and Rai, M. (2008) Exploitation of *Aspergillus niger* for synthesis of silver nanoparticles. *J Biobased Mater Bioenergy* **2**, 243–247.

Garber, G. (2001) An overview of fungal infections. *Drugs* **61** (Suppl 1), 1–12.

Gaumet, M., Vargas, A., Gurny, R. and Delie, F. (2008) Nanoparticles for drug delivery: the need for precision in reporting particle size parameters. *Eur J Pharm Biopharm* **69**, 1–9.

Gupta, A.K. and Cooper, E.A. (2008) Update in antifungals therapy of dermatophytosis. *Mycopathologia* **166**, 353–367.

Hasell, T., Yang, J., Wang, W., Brown, P. and Howdle, S. (2007) A facile synthetic route to aqueous dispersions of silver nanoparticles. *Mater Lett* **61**, 4906–4910.

Havlickova, B., Czaika, V.A. and Friedrich, M. (2008) Epidemiological trends in skin mycoses worldwide. *Mycoses* **51**(Suppl. 4), 2–15.

Hemath, N.K.S., Kumar, G., Karthik, L. and Bhaskara, R.K.V. (2010) Extracellular biosynthesis of silver nanoparticles using the filamentous fungus *Penicillium* sp. *Arch Appl Sci Res* **2**, 161–167.

Hwang, I., Lee, J., Hwang, J.H., Kim, K.-J. and Lee, D.G. (2012) Silver nanoparticles induce apoptotic cell death in *Candida albicans* through the increase of hydroxyl radicals. *FEBS J* **279**, 1327–1338.

Ingle, A., Gade, A., Pierrat, S., Sonnichsen, C. and Rai, M. (2008) Mycosynthesis of silver nanoparticles using the fungus *Fusarium acuminatum* and its activity against some human pathogenic bacteria. *Curr Nanosci* **4**, 141–144.

Jung, W.K., Koo, H.C., Kim, K.W., Shin, S., Kim, S.H. and Park, Y.H. (2008) Antibacterial activity and mechanism of action of the silver ion in *Staphylococcus aureus* and *Escherichia coli*. *Appl Environ Microbiol* **74**, 2171–2178.

Khan, A., Ahmad, A., Manzoor, N. and Khan, L.A. (2010) Antifungal activities of *Ocimum sanctum* essential oil and its lead molecules. *Nat Prod Commun* **5**, 345–349.

Kim, J.S., Kuk, E., Yu, K.N., Kim, J.H., Park, S.J., Lee, H.J., Jeong, D.H. and Cho, M.H. (2007) Antimicrobial effects of silver nanoparticles. *Nanomedicine* **3**, 95–101.

Kim, K.-J., Sung, W.S., Moon, S.-K., Choi, J.-S., Kim, J.G. and Lee, D.G. (2008) Antifungal effect of silver nanoparticles on dermatophytes. *J Microbiol Biotechnol* **18**, 1482–1484.

Kittler, S., Greulich, C., Gebauer, J.S., Diendorf, J., Treuel, L., Ruiz, L., Gonzalez-Calbet, J.M., Vallet-Regi, M. *et al.* (2010) The influence of proteins on the dispersability and cell-biological activity of silver nanoparticles. *J Mater Chem* **20**, 512–518.

Kumar, A.S., Abyaneh, M.K., Sulabha, G.S., Ahmad, A. and Khan, M.I. (2007) Nitrate reductase mediated synthesis of silver nanoparticles from $AgNO_3$. *Biotechnol Lett* **29**, 439–445.

Kvitek, L., Panacîek, A., Soukupova, J., Kolar, M., Vecîerova, R., Prucek, R., Holecova, M. and Zboril, R. (2008) Effect of surfactants and polymers on stability and antibacterial activity of silver nanoparticles (NPs). *J Phys Chem C* **112**, 5825–5834.

Kvitek, L., Vanickova, M., Panáček, A., Soukupova, J., Dittrich, M., Valentova, E., Prucek, R., Bancirova, M. *et al.* (2009) Initial study on the toxicity of silver nanoparticles (NPs) against *Paramecium caudatum*. *J Phys Chem C* **113**, 4296–4300.

Lakowicz, J.R. (2006) *Principles of Fluorescence Spectroscopy*, 3rd edn. New York: Springer Science+Business Media, LLC.

Lee, H.J., Yeo, S.Y. and Jeong, S.H. (2003) Antibacterial effect of nanosized silver colloidal solution on textile fabrics. *J Mater Sci* **38**, 2199–2204.

Li, X., Xu, H., Chen, Z.-S. and Chen, G. (2011) Biosynthesis of nanoparticles by microorganisms and their applications. *J Nanomater* **1**, 1–16.

Lok, C.-N., Ho, C.-M., Chen, R., He, Q.-Y., Yu, W.-Y., Sun, H., Tam, P.K.-H., Chiu, J.-F. *et al.* (2007) Silver nanoparticles: partial oxidation and antibacterial activities. *J Biol Inorg Chem* **12**, 527–534.

Maliszewska, I. (2011) Microbial synthesis of metal nanoparticles. In *Metal Nanoparticles in Microbiology* ed. Rai, M. and Durán, N. pp 153–175. Berlin Heidelberg: Springer-Verlag.

Mandal, D., Bolander, M.E., Mukhopadhyay, D., Sarkar, G. and Mukherjee, P. (2006) The use of microorganisms for the formation of metal nanoparticles and their application. *Appl Microbiol Biotechnol* **69**, 485–492.

Marambio-Jones, C. and Hoek, E.M.V. (2010) A review of the antibacterial effects of silver nanomaterials and potential implications for human health and the environment. *J Nanopart Res* **12**, 1531–1551.

Marcato, P.D., Durán, M., Huber, S.C., Rai, M., Melo, P.S., Alves, O.L. and Durán, N. (2012) Biogenic silver nanoparticles and its antifungal activity as a new topical transungual drug. *J Nano Res* **20**, 99–107.

Mirmirani, P., Hessol, N.A., Maurer, T.A., Berger, T.G., Nguyen, P., Khalsa, A., Gurtman, A., Micci, S. *et al.* (2001) Prevalence and predictors of skin disease in the Women's Interagency HIV Study (WIHS). *J Am Acad Dermatol* **44**, 785–788.

Monteiro, D.R., Gorup, L.F., Silva, S., Negri, M., de Camargo, E.R., Oliveira, R., Barbosa, D.B. and Henriques, M. (2011) Silver colloidal nanoparticles: antifungal effect against adhered cells and biofilms of *Candida albicans* and *Candida glabrata*. *Biofouling* **27**, 711–719.

Mukherjee, P.K., Leidich, S.D., Isham, N., Leitner, I., Ryder, N.S. and Ghannoum, M.A. (2003) Clinical *Trichophyton rubrum* strain exhibiting primary resistance to terbinafine. *Antimicrob Agents Chemother* **47**, 82–86.

Mukherjee, P., Roy, M., Mandal, B.P., Dey, G.K., Mukherjee, P., Ghatak, J., Tyagi, A.K. and Kale, S.P. (2008) Green synthesis of highly stabilized nanocrystalline silver particles by a non-pathogenic and agriculturally important fungus *T. asperellum*. *Nanotechnology* **19**, 103–110.

Mulvaney, P. (1996) Surface plasmon spectroscopy of nanosized metal particles. *Langmuir* **12**, 788–800.

Nasrollahi, A., Pourshamsian, K. and Mansourkiaee, P. (2011) Antifungal activity of silver nanoparticles on some of fungi. *Int J Nano Dim* **1**, 233–239.

Nir-Paz, R., Elinav, H., Pierard, G.E., Walker, D., Maly, A., Shapiro, M., Barton, R.C. and Polacheck, I. (2003) Deep infection by *Trichophyton rubrum* in an immunocompromised patient. *J Clin Microbiol* **41**, 5298–5301.

Noorbakhsh, F. (2011) Antifungal effects of silver nanoparticle alone and with combination of antifungal drug on dermatophyte pathogen *Trichophyton rubrum*. *Inter Conf Biosci Biochem Bioinf* **5**, 364–367.

Pal, S., Tak, Y.K. and Song, J.M. (2007) Does the antibacterial activity of silver nanoparticles depend on the shape of the nanoparticle? A study of the gram-negative bacterium *Escherichia coli*. *Appl Environ Microbiol* **73**, 1712–1720.

Panáček, A., Kolař, M., Večeřová, R., Prucek, R., Soukupová, J., Kryštof, V., Hamal, P., Zbořil, R. *et al.* (2009) Antifungal activity of silver nanoparticles against *Candida* spp. *Biomaterials* **30**, 6333–6340.

Pastoriza-Santos, I. and Liz-Marzán, L.M. (2009) *N,N*-Dimethylformamide as a reaction medium for metal nanoparticle synthesis. *Adv Funct Mater* **19**, 679–688.

Pereira, L., Dias, N., Santos, C. and Lima, N. (2014) The use of MALDI-TOF ICMS as an alternative tool for *Trichophyton rubrum* identification and typing. *Enferm Infecc Microbiol Clin* **32**, 11–17.

Racles, C., Airinei, A. and Stoica, I. (2010) Silver nanoparticles obtained with a glucose modified siloxane surfactant. *J Nanopart Res* **12**, 2163–2177.

Rai, M., Yadav, A. and Gade, A. (2009) Silver nanoparticles as a new generation of antimicrobials. *Biotechnol Adv* **27**, 76–83.

Rai, M., Gade, A. and Yadav, A. (2011) Biogenic nanoparticles: an introduction to what they are, how they are synthesized and their applications. In *Metal Nanoparticles in Microbiology* ed. Rai, M. and Durán, N. pp 1–14. Berlin, Heidelberg: Springer-Verlag.

Rajarathinam, M. and Kalaichelvan, P.T. (2013) Biogenic nanosilver as a potential antibacterial and antifungal additive to commercially available dish wash and hand wash for an enhanced antibacterial and antifungal activity against selected pathogenic strains. *Int Res J Pharm* **4**, 68–75.

Reidy, B., Haase, A., Luch, A., Dawson, K.A. and Lynch, I. (2013) Mechanisms of silver nanoparticle release, transformation and toxicity: a critical review of current knowledge and recommendations for future studies and applications. *Materials* **6**, 2295–2350.

Santos, C., Lima, N., Sampaio, P. and Pais, C. (2011) Matrix-assisted laser desorption/ionization time-of-flight intact cell mass spectrometry (MALDI-TOF-ICMS) to detect emerging pathogenic *Candida* species. *Diagn Microbiol Infect Dis* **71**, 304–308.

Seabra, A.B. and Durán, N. (2010) Nitric oxide-releasing vehicles for biomedical applications. *J Mater Chem* **20**, 1624–1637.

Sing, S., Patel, P., Jaiswal, S., Prabhune, A.A., Raman, C.V. and Prasad, B.L.V. (2009) A direct method for the preparation of glycolipid–metal nanoparticle conjugates: sophorolipids as reducing and capping agents for the synthesis of water re-dispersible silver nanoparticles and their antibacterial activity. *New J Chem* **33**, 646–652.

Singh, M., Singh, S., Prasad, S. and Gambhir, I.S. (2008) Nanotechnology in medicine and antibacterial effect of silver nanoparticles. *Dig J Nanomater Biostruct* **3**, 115–122.

Sondi, I. and Salopek-Sondi, B. (2004) Silver nanoparticles as antimicrobial agent: a case study on *E. coli* as a model for Gram-negative bacteria. *J Colloid Interface Sci* **275**, 177–182.

Sui, X., Yuan, J., Yuan, W. and Zhou, M. (2008) Preparation of cellulose nanofibers/nanoparticles via electrospray. *Chem Lett* **37**, 114–115.

Thakkar, K.N., Mhatre, S.S. and Parikh, R.Y. (2010) Biological synthesis of metallic nanoparticles. *Nanomedicine* **6**, 257–262.

Toshijazu, T. (1999) Antimicrobial agent composed of silica-gel with silver complex. *Inorg Mater* **6**, 505–511.

Tran, Q.H., Nguyen, V.Q. and Le, A.-T. (2013) Silver nanoparticles: synthesis, properties, toxicology, applications and perspectives. *Adv Nat Sci Nanosci Nanotechnol* **4**, 033001.

Tu, W. (2008) Study on the interaction between polyvinylpyrrolidone and platinum metals during the

formation of the colloidal metal nanoparticles. *Chin J Polym Sci* **26**, 23–29.

Vigneshwaran, N., Ashtaputre, N.M., Varadarajan, P., Nachane, R.P., Paralikar, K.M. and Balasubramanya, R.H. (2007) Biological synthesis of silver nanoparticles using the fungus *Aspergillus flavus*. *Mater Lett* **61**, 1413–1418.

Wang, H., Qiao, X., Chen, J. and Ding, S. (2005) Preparation of silver nanoparticles by chemical reduction method. *Colloids Surf B Biointerfaces* **256**, 111–115.

Xu, W., Cooper, E.I. and Angell, A.C. (2003) Ionic liquids: ion mobilities, glass temperatures, and fragilities. *J Phys Chem B* **107**, 6170–6178.